

Copyright 2001, Society of Photo-Optical Instrumentation Engineers
This paper was given at SPIE's 26th Annual International Symposium on
Microlithography, presentation number 4345-118 and is made available as an electronic
reprint with permission of SPIE. One print or electronic copy may be made for personal
use only. Systematic or multiple reproduction, distribution to multiple locations via
electronic or other means, duplication of any material in this paper for a fee or for
commercial purposes, or modification of the content of the paper are prohibited.

Modeling the impact of thermal history during post exposure bake on the lithographic performance of chemically amplified resists

Mark D. Smith^{a*}, Chris A. Mack^{a*}, John S. Petersen^{b**}
^aKLA-Tencor Corp., ^bPetersen Advanced Lithography, Inc.

ABSTRACT

In this study, the influence of the thermal history during post exposure bake (PEB) on the lithographic performance of a chemically amplified resist is examined using a reaction-diffusion model of the resist combined with an arbitrary time-temperature profile. The temperature profiles investigated in this study are either based on a simple heat transfer model or arbitrary time-temperature data. The heat transfer model allows variation of the rise time to the bake temperature, of the cooling process during transfer to the chill plate, and of the fall time to the chill plate temperature. Calculations of the dose-to-size for dense features and the iso-dense bias are presented for typical temperature profiles, and these results are contrasted with the lithographic responses for an “ideal” bake. Also, the lithographic response for a double bake is presented. For certain resist model parameters, the lithographic response for a higher temperature bake followed by a lower temperature bake can be significantly different from the response when the lower temperature bake precedes the higher temperature bake.

Keywords: hotplate, heat transfer, double bake, PROLITH, lithography simulation

1. INTRODUCTION

As device sizes continue to shrink, the lithography process becomes increasingly sensitive to process perturbations. A standard practice in all manufacturing environments is to periodically run a focus-exposure matrix in order to determine the size of the exposure process window – for a large process window, the process will be less sensitive to perturbations to the focal position and exposure dose. Of course, perturbations to process steps other than aerial image formation can be detrimental to the quality of the final pattern in resist. Chemically amplified resists require both an exposure dose to generate a latent acid image and a thermal dose to drive the deblocking reaction that changes the solubility of the resist in developer. Because the photogenerated acid diffuses through the resist as it catalyzes the deblocking reaction, the acid could diffuse into unexposed regions and have a significant impact on the quality of the image generated in the resist. A successful post-exposure bake (PEB) process must optimize the balance between the relative rates of the diffusion and reaction processes, and because the diffusivity and the reaction rate are both temperature dependent, careful attention to the thermal history of the resist may be required.

In this study, the influence of the thermal history during PEB on the lithographic performance of a chemically amplified resist is examined using PROLITH version 7.0. The PEB model in PROLITH version 7.0 is a reaction-diffusion model of the resist combined with an arbitrary time-temperature profile. The temperature profiles investigated in this study are either based on a simple heat transfer model or on a text file containing time-temperature data. The heat transfer model allows variation of the rise time to the bake temperature, of the ambient cooling process

* mark.d.smith@kla-tencor.com; phone 1-512-381-2318; 8834 North Capital of Texas Highway, Suite 301, Austin, TX 78759; ** jpetersen@advlitho.com; phone 1-512-241-1100; 8834 North Capital of Texas Highway, Suite 304, Austin, TX 78759

during transfer to the chill plate, and of the fall time to the chill plate temperature. A typical time-temperature profile is shown in Figure 1. Temperature profiles imported from a text file allow an arbitrary thermal history that is not described by the heat transfer model. For example, one could import a double bake profile, similar to the one shown in Figure 2, or import experimentally measured hotplate data.

The results in this investigation are presented in two parts. First, the influence of a finite rise time to the hotplate temperature on the resist CD is investigated for both isolated and dense features. A similar analysis is performed to determine the impact of transfer delays between the hotplate and the chillplate. In the second part of the study, the lithographic response for a double bake is presented. For certain resist model parameters, the iso-dense bias for a higher temperature bake followed by a lower temperature bake can be significantly different from the response when the lower temperature bake precedes the higher temperature bake. These results are in agreement with the experimentally observed trends [1] for double bakes of chemically amplified resists.

2. HOTPLATE AND RESIST MODELS FOR PEB

We simulate the temperature profile on a typical track system with a three-stage model for heat transfer to the resist-coated wafer [2,3,4]. The three stages in this model are proximity hotplate, transfer from the hotplate to the chillplate, and then proximity cooling on the chillplate. During each of these stages, the temperature of the wafer is described by the following differential equation

$$\rho C_p L \frac{dT}{dt} = -\frac{k_{air}}{\delta} (T - T_{plate}) - h(T - T_{ambient}) \quad (1)$$

where ρ is the density of silicon, C_p is the heat capacity of silicon, L is the thickness of the wafer, T is the temperature of the resist-coated wafer, k_{air} is the thermal conductivity of air, δ is the thickness of the gap between the hotplate or chillplate and the wafer, and h is a heat transfer coefficient for heat lost from the top surface of the wafer to the surroundings. In this model, the term on the left side represents the thermal mass of the wafer, and the terms on the right side represent heat transfer on the bottom side of the wafer from the hotplate and heat loss from the top of the wafer to the surroundings. During the second stage where the wafer is transferred from the hotplate to the chillplate, the gap δ is assumed to be very large so that the first term on the right side of Eq. (1) is unimportant, and the second term on the right side is assumed to represent heat loss from the top and bottom wafer surfaces.

The solution to the heat transfer model given described by Eq. (1) is

$$T = (T_{initial} - T^*) \exp\left(-\frac{t}{\tau}\right) + T^* \quad (2)$$

where $T_{initial}$ is the temperature at the beginning of the stage, T^* is the equilibrium temperature given by

$$T^* = \frac{\frac{k_{air}}{\delta} T_{plate} + h T_{ambient}}{\frac{k_{air}}{\delta} + h} \quad (3)$$

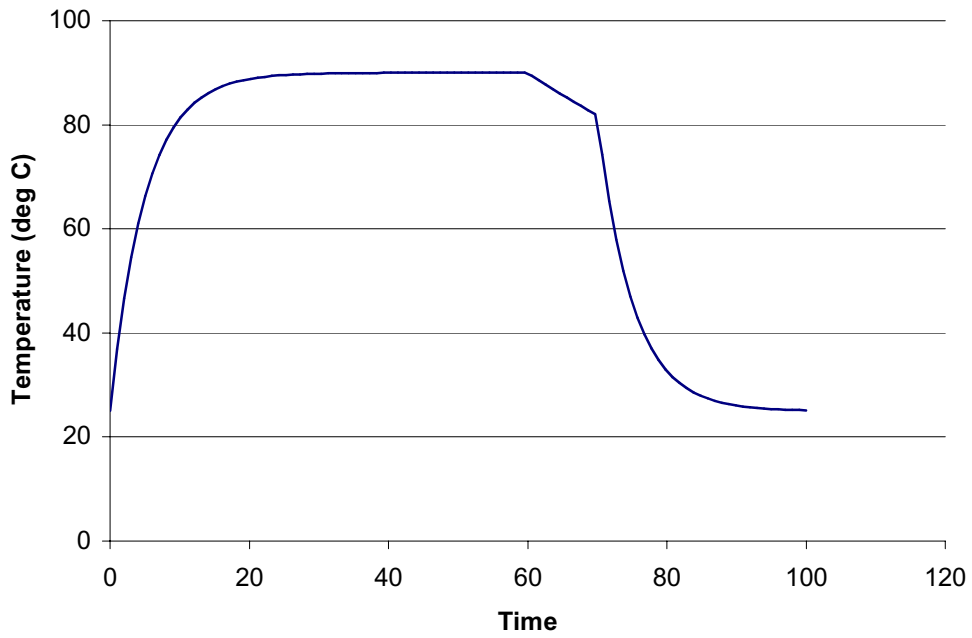


Figure 1: Temperature profile described by a three-stage heat-transfer model of a proximity bake.

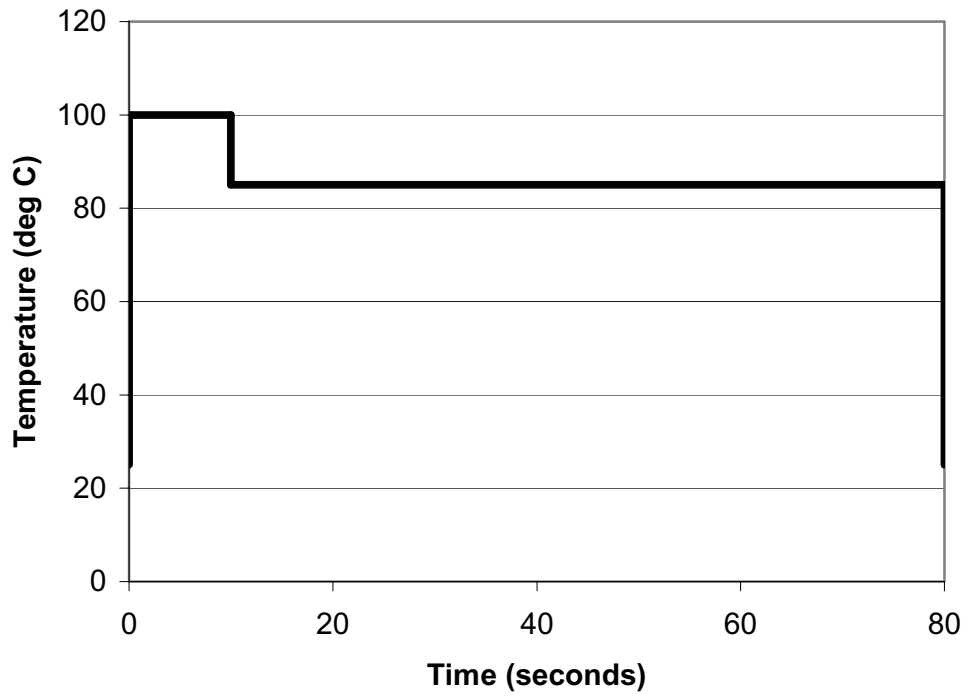


Figure 2: Double bake temperature profile. The first bake is at 100 C for 10 seconds, and the second bake is at 85 C for 70 seconds.

and τ is the time constant for heating or cooling the wafer,

$$\tau = \frac{\rho C_p L}{\frac{k_{air}}{\delta} + h} \quad (4)$$

It is interesting to note that the equilibrium temperature T^* is not equal to the temperature of the hotplate, as shown by Eq. (3). The fact that the equilibrium temperature of the wafer is usually very close to the hotplate temperature indicates that heating across the gap is the dominant heat transfer mechanism. This is because the gap spacing δ is very small, typically about 0.15 mm. Even if significant variations in δ across the wafer are present, the value of T^* will still be dominated by the temperature of the hotplate, and good temperature uniformity can be achieved.

By contrast, variations in the gap spacing can have a large effect on the time constant τ , as demonstrated by Eq. (4). Variations in the gap spacing can be due to misalignment of the ceramic pins that control the gap spacing in the proximity plate, or due to non-flatness of the silicon wafer – the warp of a 200 mm wafer can be up to 0.076mm [3,5]. In order to obtain a worst-case estimate for the variations in the time constant τ , we assume that the heat transfer is entirely due to the proximity gap ($h=0$). For the case where the warp of the wafer makes the gap smaller, the time constant is reduced by a factor of two, while for the case where the wafer makes the gap larger, the time constant increases by a factor of 1.5. We will return to this estimate for the variations in τ when we investigate the influence of temperature variations across the wafer on exposure latitude.

Although the equilibrium temperatures given by Eq. (3) and the time constants given by Eq. (4) can be calculated from measurable quantities, it is often most useful to fit these parameters to experimental data. The parameter values given in Table 1 are typical for a proximity bake process, and these values were used to generate the temperature profile shown in Figure 1.

We use a model for APEX-E in our study of the temperature profiles during PEB. APEX-E was chosen for its poor PEB sensitivity, which is defined as the linewidth variation due to a change in the PEB bake temperature. The PEB sensitivity of APEX-E has been measured to be 16.2 nm/°C [6]. The parameters for our model of APEX-E are given in Table 2, and PROLITH simulations with these values reproduce the dose-to-size and PEB sensitivity observed experimentally by Kemp, et al. [6]. Furthermore, the iso-dense bias calculated for annular illumination with this model for 250.0 nm features is -55.0 nm, which is in good agreement with measured values [7]. (When calibrating the model, an ideal hotplate temperature profile for the PEB was assumed.) Throughout the rest of the paper, we simulate 762 nm of APEX-E on silicon with an imaging tool similar to that used by Kemp: annular illumination with $\sigma_{inner}=0.45$, $\sigma_{outer}=0.75$, and $NA=0.54$.

Stage	Equilibrium Temperature, T^* (°C)	Time Constant, τ (sec)	Duration (sec)
Hotplate	90.0	5.0	60.0
Transfer	45.0	50.0	10.0
Chillplate	25.0	5.0	30.0

Table 1. Parameters for the lumped capacitance model used to generate the temperature profile shown in Figure 1. The initial temperature for the transition stage and the chillplate stage is calculated as the temperature at the end of the previous stage.

<u>PEB Model</u>	<u>Exposure Dill Parameters</u>	<u>Mack Develop Model</u>
Diffusivity, $\ln(Ar) = 53.16 \text{ nm}^2/\text{sec}$	$A = 0.0 \text{ } \mu\text{m}^{-1}$	$R_{\text{max}} = 134.0 \text{ nm}/\text{sec}$
Diffusivity, $E_a = 35.68 \text{ kcal}/\text{mol}$	$B = 0.3620 \text{ } \mu\text{m}^{-1}$	$R_{\text{min}} = 0.4 \text{ nm}/\text{sec}$
Amplification, $\ln(Ar) = 48.09 \text{ sec}^{-1}$	$C = 0.0159 \text{ cm}^2/\text{mJ}$	$M_{\text{th}} = 0.3$
Amplification, $E_a = 35.68 \text{ kcal}/\text{mol}$		$n = 5.2$
Acid loss, $\ln(Ar) = 2.986 \text{ sec}^{-1}$		
Acid loss, $E_a = 4.986 \text{ kcal}/\text{mol}$		
Relative Quencher = 0.03		
Room temperature diffusion: 20.0 nm		

Table 2: Resist model parameters for APEX-E.

3. INFLUENCE OF THERMAL HISTORY ON FEATURE DIMENSIONS

The importance of the thermal history on feature dimensions is demonstrated by comparing the dose-to-size required for an ideal bake with the more realistic temperature profile shown in Figure 1. For 250 nm lines and spaces, the dose-to-size for an ideal bake of 90 °C for 60 seconds is calculated as 15.1 mJ/cm², whereas the calculated dose-to-size is 18.0 mJ/cm² when using the 3-stage heat transfer model given in Table 1. The difference in the required exposure dose indicates that the temperature profile shown in Figure 1 represents a smaller thermal dose than the ideal bake, so a 20% larger exposure dose is required.

Qualitatively, one might associate the area under the temperature profile curve with the size of the thermal dose, and based on the shape of the temperature profile in Figure 1, it is not immediately obvious why the new hotplate model leads to a decrease in the thermal dose. On one hand, the finite rise time to the bake temperature should decrease the thermal dose, but on the other hand, the slow cooling of the wafer during the transfer step should increase the thermal dose. The impact of each of these parameters in the model is easily determined by performing quantitative calculations where each parameter is varied while keeping the other parameters fixed. The first set of results is shown in Figure 3 where feature dimensions are shown for isolated and dense features as a function of rise time to the bake temperature. All remaining parameters in the hotplate model are given in Table 1. As shown in the figure, the dense features scum for rise times larger than 7 seconds, while the size of the isolated line increases almost linearly with rise time.

The influence of the duration of the transfer from the hotplate to the chillplate on feature dimensions is shown in Figure 4. As for the calculation for rise time to the hotplate temperature, the exposure dose is 18.0 mJ/cm², and all of the parameters in the hotplate model other than the duration of the transfer remain fixed at the values given in Table 1. The results in the figure demonstrate the impact of transfer delays on the PEB process – if the end of the bake arrives and the proximity pins come up, and the track robot is temporarily unavailable, a transfer delay can occur. By contrasting the responses shown in Figures 3 and 4, it is apparent that the CD is more sensitive to the rise time than to transfer delays. This is demonstrated by the fact that the slopes of the curves in Figure 3 at a rise time of 5 seconds (the rise time in the baseline process) are larger in magnitude than the slopes of the curves in Figure 4 at the baseline value of the transfer duration, 10 seconds. However, for both cases, dense features are more sensitive to perturbations to the thermal history than isolated features.

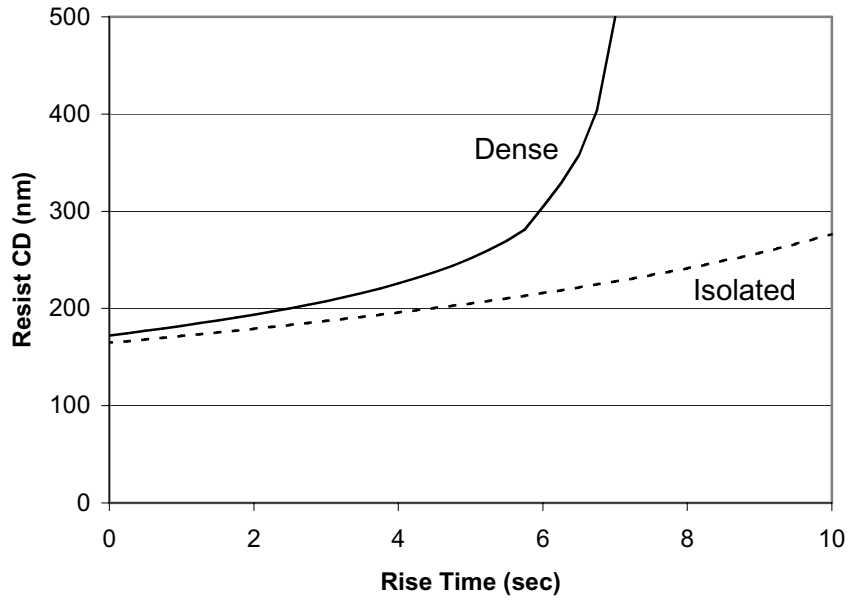


Figure 3: Resist CD for isolated and dense lines as a function of the rise time to the hotplate temperature. Isolated features are shown with the dashed curve, and dense features are shown with the solid curve.

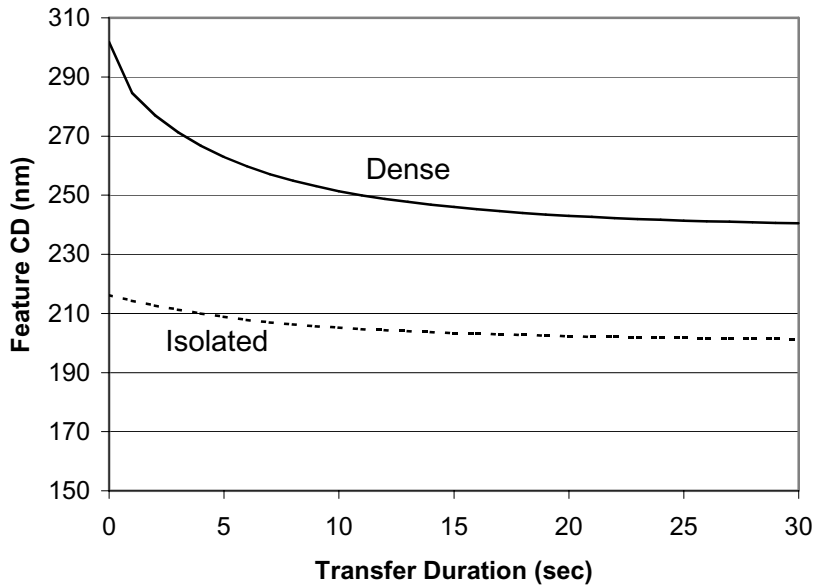


Figure 4: Resist CD for isolated and dense lines as a function of the duration of the transfer step from the hotplate to the chillplate. Isolated features are shown with the dashed curve, and dense features are shown with the solid curve.

These results are all consistent with the fact that the 3-stage hotplate model corresponds to a smaller thermal dose than the ideal hotplate model. However, the relationship between the thermal dose and the temperature profile is also influenced by the temperature dependence of the model parameters for APEX-E. In the model described in Table 2, there are three activated processes: diffusion, the amplification reaction, and the acid loss reaction. The activation energies for diffusion and the amplification reaction are both high (35.68 kcal/mol) whereas the activation energy for the loss reaction is low (4.986 kcal/mol). This indicates that the rate of the acid loss reaction will be relatively constant compared with the temperature dependence of diffusion and amplification. Therefore, at early times in the bake, acid will be lost before the wafer is hot enough to activate the diffusion and amplification processes. This theory can be tested by increasing the activation energy of the loss reaction to 35.68 kcal/mol and increasing the pre-exponential value to $\ln(Ar)=45.554$. With these choices, the acid loss rate constant has the same value at 90 °C, $k_{loss}=0.0197 \text{ sec}^{-1}$, but the temperature dependence is the same as for the diffusivity and amplification reaction rate constant. With this new model for the acid loss reaction, the dose-to-size for dense features remains unchanged for the ideal bake (15.1 mJ/cm²), but the dose-to-size changes from 18.0 mJ/cm² to 16.0 mJ/cm² for the 3-stage hotplate model. Thus, the temperature dependence of the acid loss reaction can account for two-thirds of the change in the required dose.

When this result is combined with the results in Figures 3 and 4, the following description of the 3-stage bake process emerges: at the beginning of the bake, the acid loss reaction scavenges acid before the wafer reaches a temperature that is hot enough to drive the deblocking reaction. After the hotplate temperature is reached, acid loss, diffusion, and amplification occur simultaneously. Finally, during the transfer to the chillplate, the temperature of the wafer decreases and the amplification and diffusion processes cease and only the acid loss process continues. Therefore, delays in reaching the bake temperature can result in substantial acid loss before deblocking can begin, and transfer delays are relatively unimportant because the amplification reaction is quickly shut-down at the end of the bake, regardless of the duration of the transfer stage.

Bearing the above conclusions in mind, we anticipate that the perturbations to the rise time during the bake could possibly have a large impact on the process window for chemically amplified resists. As outlined in Section 3, changes in the rise time by a factor of two might occur due to non-flatness of the wafer. In Figure 5, process windows are shown for hotplate rise times of 2.5 and 5.0 seconds, and as demonstrated by the figure, perturbations to the rise can lead to a substantial decrease in the usable portion of the focus-exposure process window.

For the last set of calculations in this study, we will compare the iso-dense bias obtained when simulating a double bake profile, as shown in Figure 2. We examine two double bake temperature profiles: in the first bake profile, the first part of the bake is a higher temperature bake at 100 °C for 10 seconds, and the second part is a lower temperature bake at 85 °C for 70 seconds. For the second double bake profile, the lower temperature bake precedes the higher temperature bake. Although the total area under the temperature profile curves is the same, the effective thermal doses are different. This is demonstrated by the dose-to-size values for dense-features, given in Table 3. From these values, we conclude that the effective thermal dose is larger when the higher temperature bake is first. Again, this is due to the temperature dependence of the acid loss reaction – when the lower temperature bake is first, the rate of the acid loss reaction is relatively unchanged, but the amplification reaction is much slower due to the lower temperature, and by the end of the lower temperature bake, much of the acid has been consumed. When the higher temperature bake is first, the rate of the amplification reaction is greatly increased, and so more

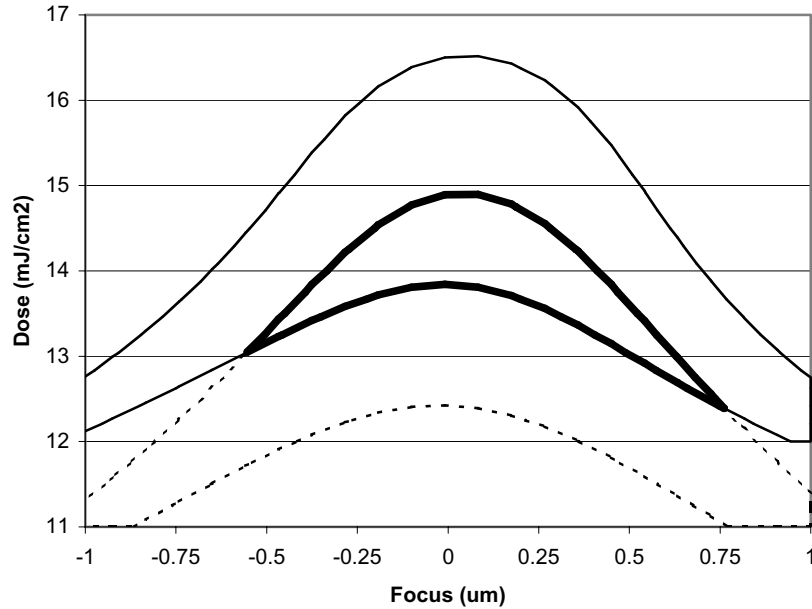


Figure 5: Process windows for isolated lines with a hotplate rise time of 2.5 seconds (dashed curve) and a hotplate rise time of 5.0 seconds (solid curve). The overlapping portion of the process window is shown in bold.

	Dose to size (mJ/cm ²)	CD Isolated Lines (nm)	Iso-Dense Bias (nm)
100 C/ 85 C	12.0	211	-39
85 C/ 100 C	17.2	203	-47

Table 3: Calculated dose-to-size for dense features and iso-dense bias values for double bakes with APEX-E.

deblocking can occur relative to the rate of the acid loss reaction. The iso-dense bias changes with the order of the double bake as well. As before, we can make the activation energy of the loss reaction equal to the activation energy of the diffusivity and the amplification reaction without changing the rate at 90 °C (i.e., choose $\ln(Ar)=45.554$ for the loss reaction). For this case, the dose-to-size and iso-dense bias are the same for both double bakes, 14.3 mJ/cm² and -43nm, respectively, and the two double bakes are lithographically identical.

4. SUMMARY AND CONCLUSIONS

We have used PROLITH version 7.0 to simulate arbitrary temperature profiles during PEB for chemically amplified resists. For a simple heat transfer model that reproduces the salient features of a proximity bake, we found that the resulting resist profiles were sensitive to the rise time to the hotplate bake temperature. The model of APEX-E used in this study has high activation energies for the diffusion and amplification reaction processes and a low activation energy for the acid loss reaction. Thus, delays in reaching the bake temperature could lead to substantial acid

loss before the deblocking reaction could begin. As a result, bake profiles with long rise times to the bake temperature required a larger exposure dose in order to generate a larger initial concentration of acid. From a process control standpoint, this means that small variations in the rise time to the hotplate temperature can lead to significant shrinkage of the focus-exposure process window. By contrast, variations in the duration of the transfer time between the hotplate and the chillplate were not as important in determining the final resist CDs, though still significant.

Double bake temperature profiles were also investigated, and we found that larger exposure doses were required for double bakes consisting of a lower temperature bake followed by a higher temperature bake, as compared to double bakes where the higher temperature bake was first. As found experimentally [1], the iso-dense bias was also different for the two double bakes. Again, the most important parameters in our model were the relative magnitude of the activation energies for acid loss, diffusion, and amplification reaction. When the model was re-formulated so that the activation energies were all equal, the two double bakes were lithographically equivalent.

This work demonstrates that variations in the temperature profiles during PEB can have a significant impact on the final resist CD and shrink the focus-exposure process window. While the first half of this paper emphasized the negative impact of perturbations to the temperature profile on the focus-exposure process window, the investigation of the influence of double bakes on iso-dense bias emphasizes the possibility of manipulating the distribution of CDs by engineering the shape of the time-temperature profile, as described by Petersen, et al. [1]. Of course, the specific conclusions presented here will depend on the parameters assumed for the resist model, but in general, whenever the activation energies of competing reactions are different, the details of the time-temperature profile during PEB can have a significant impact on the final resist profiles. This conclusion emphasizes the need for accurate estimates of both the magnitude of the rate constants and the corresponding activation energies.

5. ACKNOWLEDGEMENTS

The authors would like to thank Jeffrey D. Byers for many helpful discussions and for supplying resist parameters for APEX-E.

6. REFERENCES

- 1) J.S. Petersen, J.D. Byers, and R.A. Carpio, "The formation of diffusion wells in acid catalyzed photoresists" *Microelectronic Engineering*, 35 (1997) 169-174.
- 2) D.P. DeWitt, T.C. Niemoeller, C.A. Mack, G. Yetter, "Thermal design methodology of hot and chill plates for Microlithography" *Proc. SPIE*, 2196 (1994) 432-448.
- 3) N. Ramanan, F.F. Liang, J.B. Sims, "Conjugate heat-transfer analysis of 300-mm bake station" *Proc. SPIE*, 3678 (1999) 1296-1306.
- 4) Y.M. Lee, M.G. Sung, E.M. Lee, Y.S. Sohn, H.J. Bak, H.K. Oh, "Temperature rising effect of 193 nm chemically amplified resist during post exposure bake" *Proc. SPIE*, 3999 (2000) 1000-1008.
- 5) SEMI Standard M1.9-91, "Standard for 200mm polished monocrystalline silicon wafers" SEMI North America, Mountain View, California.
- 6) K. Kemp, D. Williams, J. Cayton, P. Steege, S. Slonaker, R. Elliot, "Effects of DUV sensitivities of lithographic process window" *Proc. SPIE*, 3049 (1997) 955-962.
- 7) N. Thane, R. Savage II, D. Stark, L. Hollifield, "Reaching for 0.25 μ m with current available tool set" *Proc. SPIE*, 2439 (1995) 89-103.